LBL-25908 c.1
Preprint

Lawrence Berkeley Laboratory

UNIVERSITY OF CALIFORNIA

Physics Division

Submitted to Physical Review D

A Practical Laboratory Detector for Solar Axions

K. van Bibber, P.M. McIntyre, D.E. Morris,
and G.G. Raffelt

September 1988

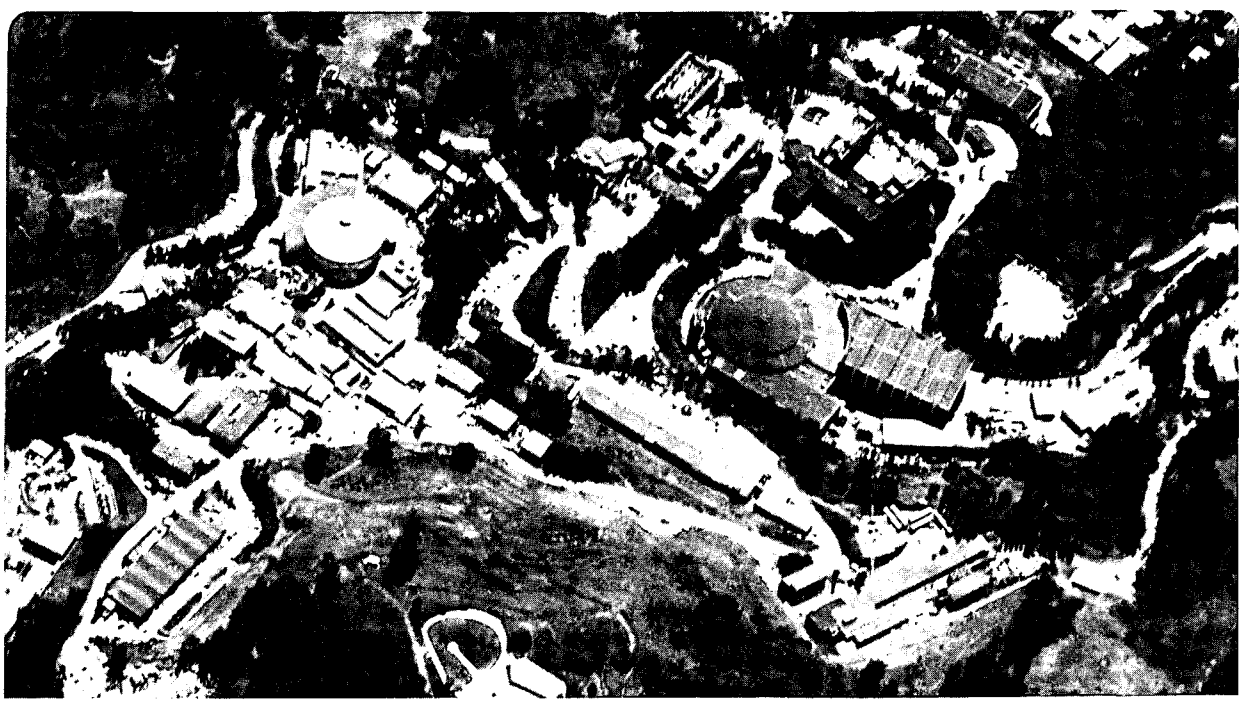

Prepared for the U.S. Department of Energy under Contract Number DE-AC03-76SF00098.

DISCLAIMER

A Practical Laboratory Detector for Solar Axions

K. van Bibber[1], P.M. McIntyre[2], D. E. Morris[3], and G.G. Raffelt[4,5]

[1]*Physics Department, Lawrence Livermore National Laboratory, University of California*
Livermore, CA 94550

[2]*Physics Department, Texas A&M University*
College Station, TX 77843

[3]*Physics Division, Lawrence Berkeley Laboratory,*
1 Cyclotron Road,
Berkeley, CA 94720

[4]*Institute for Geophysics and Planetary Physics, Lawrence Livermore National Laboratory,*
University of California
Livermore, CA 94550

[5]*Astronomy Department, University of California*
Berkeley, CA 94720

September 7, 1988

ABSTRACT

We present a practical design for a detector sensitive to axions and other light particles with a two-photon interaction vertex. Such particles would be produced in the solar interior by Primakoff conversion of blackbody photons and could be detected by their re-conversion into x-rays (average energy about 4 keV) in a strong laboratory magnetic field. An existing large superconducting magnet would be suitable for this purpose. The transition rate is enhanced by filling the conversion region with a buffer gas (H_2 or He). This induces an effective photon mass (plasma frequency) which can be adjusted to equal the axion mass being searched for. Axion-photon conversion is then coherent throughout the detector volume for all axion energies. Axions with mass in the range $0.1\ \text{eV} \lesssim m_a \lesssim 5\ \text{eV}$ can be detected using gas pressures of 0.1 – 300 atm. Axions with the standard coupling strength to photons would give counting rates of 10^{-5} – 10 sec^{-1} over this mass range. The search would definitively test one of the only two regions of axion parameters not excluded by astrophysical constraints.

1. Introduction

1.1 Motivation

The conservation of the CP symmetry in strong interactions has been a long standing puzzle of particle physics in view of the CP violating effects observed in the K^o meson system. In a compelling theoretical scheme proposed by Peccei and Quinn[1] the measured absence (or extreme smallness) of the neutron electric dipole moment is linked to the existence of a hitherto undetected particle — the axion[2,3]. The phenomenological properties of this light, neutral pseudoscalar are mainly determined by the Peccei-Quinn parameter (or axion decay constant) f_a which arises as the scale at which the global chiral $U(1)$ symmetry postulated by Peccei and Quinn is spontaneously broken. Although it was originally thought that f_a should be identified with the electroweak scale $f_{weak} \approx 250$ GeV (standard axions), the axion decay constant can take on, in principle, any value between the GeV range and the Planck scale of 10^{19} GeV. Since the interaction strength of axions with matter and radiation scales as $1/f_a$, axion models with $f_a >> f_{weak}$ are generically referred to as "invisible axions"[3,4,5].

Depending upon the assumed value for f_a, the existence of axions would lead to a startling variety of phenomenological consequences in particle physics, astrophysics, and cosmology. The combined evidence from these different fields now excludes large ranges of f_a values, leaving only two rather narrow windows in which axions might still exist. Thus it has become a compelling task to attempt the detection of axions in these remaining ranges of parameters, or to exclude the Peccei-Quinn mechanism once and for all as not being realized in nature.

1.2 Principle of the detector

The basic idea of this experiment, which relies on the two photon coupling of axions or other light, exotic particles was suggested by Sikivie[6]. This vertex allows for the Primakoff conversion (Fig. 1) of photons into axions in the presence of external electric or magnetic fields. Thus axions would be produced in the solar interior where blackbody photons with energies of several keV would be converted in the fluctuating electric fields of the charged particles in the hot plasma. These keV axions from the sun could reconvert into x-rays by a strong magnetic field in the laboratory ("axion helioscope"). Since the magnetic field varies only over macroscopic scales, the axion-photon conversion is best visualized as a mixing phenomenon[7] between these states in the presence of the external field: an initial axion state partly oscillates into a photon which can be detected.

The axion-photon conversion can be optimized using either of two strategies. The first strategy would employ a low-absorption buffer gas to establish coherent conversion over the entire detector volume. The axion search would be conducted as a narrow-band scan using a surface detector array. The second strategy would employ a high-absorption buffer gas to absorb and detect x-rays near the point of conversion. This volume detector would then permit a broad band axion search.

The transition rate is largest when the axion and photon amplitudes are coherent throughout the detection volume. For axions of non-zero mass, this coherence can be achieved by filling the conversion region with an appropriate medium to give the photons an effective mass m_γ which can be made to match m_a, as shown in our preliminary reports[8]. In general, of course, photons do

not follow the dispersion relation

$$k^2 = \omega^2 - m_\gamma^2 \qquad (1)$$

relevant for massive particles. However, for x-rays, when the energy of the photons is sufficiently far above all resonances, $k^2 = \omega^2 - \omega_p^2$ is an exceedingly good approximation. The role of m_γ is played by the plasma frequency $\omega_p = (4\pi\alpha N_e/m_e)^{1/2}$, where N_e is the number density of bound and free electrons. Of course, for conversion of massless bosons the degeneracy condition with photons is automatically satisfied in a vacuum, as discussed by Anselm[9].

The x-ray energy must be far above the highest resonance (ionization energy) of the buffer gas. This requirement is satisfied by hydrogen or helium. Furthermore, the absorption length for keV x-rays in H_2 or He gas is many meters (1800 m and 100 m respectively at STP for 4 keV x-rays) and is larger than the dimensions of the detector. Thus, the imaginary part of the dispersion relation does not lead to excessive absorption of the photon component of the beam. The experiment would be operated in a scanning mode in which the gas pressure is varied in appropriate steps to cover a range of possible axion masses.

In summary, the main ingredients of this detection scheme are (a) the sun as an axion source; (b) a strong magnetic field to mix the axion with the photon for reconversion; (c) a buffer gas (H_2 or He) to match the axion and photon dispersion relations and produce coherent conversion; and (d) a large area array of detectors sensitive to single photons in the 1–10 keV range, with very low background rate.

The provision for coherent conversion is limited to axion masses $m_a \lesssim 5$ eV because the gas pressure cannot be arbitrarily raised without prohibitive engineering problems. To extend the search to larger axion masses one can employ a modification of this scheme. The conversion region can be filled with a gas mixture which efficiently absorbs x-rays by the photoelectric effect. Then the photon component of the beam will be detected throughout the conversion volume. In this case the photon and axion dispersion relations do not match, but the mixture of light and heavy gases can be adjusted to provide the optimum attenuation length for x-rays to prevent destructive interference. This alternative gives a detection rate smaller than the matched dispersion scheme, but much larger than the rate from a magnetic field in a vacuum as first suggested by Sikivie[6].

1.3 Relevant parameter range

Our experiment is sensitive to at least one decade of f_a values, and covers one of the two remaining parameter ranges in which axions may still exist. It is convenient to discuss the relevant parameter ranges in terms of the axion mass m_a by virtue of a universal relationship between m_a and f_a (following the normalization conventions of Srednicki[5]),

$$m_a = 1.2 \text{ eV } N \ (10^7 \text{ GeV} / f_a), \tag{2}$$

where N is a non-zero, model-dependent integer coefficient of the color anomaly of the axion current. Note that the axion coupling to gluons, which is at the heart of the Peccei-Quinn scheme, is given as $(\alpha_s / 4\pi)\,(N / f_a)\, G\tilde{G}a$ with the strong fine structure constant α_s and the axion field a. Thus the generic parameter governing different axion models is f_a / N which is uniquely represented by the axion mass.

The axion photon interaction is given as:

$$\mathcal{L}_{a\gamma\gamma} = -\frac{1}{4M}\, a\, F_{\mu\nu}\tilde{F}^{\mu\nu} = \frac{a\,\mathbf{E}\cdot\mathbf{B}}{M}\,, \tag{3}$$

where a is the axion field, $M = \left|(\alpha/\pi)\,(N/f_a)\,(E/N - 1.92)\right|^{-1}$, and in this latter expression E is the coefficient of the electromagnetic anomaly of the axion current. Typical values of interest are m_a in the eV range and M in the 10^{10} GeV range. With the notation $M_{10} = M/10^{10}$ GeV we may express M in terms of m_a as

$$\frac{1}{M_{10}} = \frac{E/N - 1.92}{8/3 - 1.92} \times 1.45\,(m_a/\mathrm{eV})\,. \tag{4}$$

In all grand unified axion models $E/N = 8/3$, and we shall refer to this value as the GUT relationship between the axion mass and the axion photon coupling strength. Other values for E/N are possible, however, and specifically $E/N = 2$ would lead to a large suppression of the photon coupling strength[4]. For clarity we confine our discussion to GUT axions with $E/N = 8/3$ unless otherwise stated. Then our range of sensitivity is

$$0.1\ \mathrm{eV} \lesssim m_a \lesssim 5\ \mathrm{eV} \tag{5}$$

A general analysis of the experimental results would fully explore the two-dimensional (m_a, M) parameter space. Such a general discussion would also cover hypothetical massless bosons such as Sikivie's "omions"[10] and Anselm's "arions"[9,11].

1.4 Astrophysical constraints on axion parameters

Our range of sensitivity overlaps, in part, with mass ranges excluded by astrophysical arguments. However, we believe that axions can still exist in our parameter range. We discuss bounds on the axion-photon coupling from the observed lifetimes of horizontal branch stars[12], and bounds on the axion-nucleon coupling from late neutron star cooling[13,14,15] and from the supernova (SN) 1987A (Ref. 16). The entire range 0.03 eV $\lesssim m_a \lesssim$ 10 keV would seem to be excluded by the observed white dwarf cooling time scale[17], and from the suppression of helium ignition in low mass red giants[18]. However, these bounds are irrelevant if the axions do not couple to electrons at tree level ("hadronic axions"[4]) and we shall confine our attention to this type of axion.

In all axion models, there exist generic couplings to nucleons through the axion-pion mixing which is also responsible for the non-zero mass of the axion. The primary interest of our experiment is to search for axions, so we need to consider the astrophysical bounds on the axion-nucleon coupling. (For other cases such as Sikivie's omions[10] which do not couple to nucleons, these results are not relevant.) Axion emission from neutron stars by nuclear bremsstrahlung processes would lead to an observable acceleration of their cooling times[13,14,15] if $m_a \gtrsim 0.04$ eV. However, the determinations of surface temperatures of pulsars of known ages are uncertain; in fact, the existing results essentially constitute upper bounds.[19] Therefore the existence of axions with mass in our range of sensitivity is not precluded.

Observation of the neutrino pulse from the SN 1987A indicates that the gravitational binding energy released in the collapse of the progenitor star was carried away by neutrinos, limiting the interaction strength of axions and other weakly interacting, exotic particles[16]. However if axions

interact too strongly they would be "trapped" just like neutrinos in the hot proto-neutron star that forms after the collapse. This would make the axions ineffective in carrying away the energy stored in the SN core. The excluded regime translates, in a model-dependent fashion into a regime of excluded axion masses 0.001 eV $\lesssim m_a \lesssim$ 2 eV. The uncertainty of this range is substantial, perhaps as much as an order of magnitude on either end. This means that the range of axion mass that is actually excluded may be much smaller than stated.

The axion-photon coupling which is the basis of the proposed detector, allows for axion production in stellar interiors by the Primakoff effect. In a detailed discussion of stellar evolution it has been shown[12] that this exotic energy loss mechanism would lead to a severe conflict between calculated and observed lifetimes of helium burning red giants (horizontal branch stars) unless $M > 1\times10^{10}$ GeV. It is thought that the uncertainty in this bound does not exceed a small factor of order unity. This limit applies for axions lighter than about 10 keV so that their emission from the stellar plasma will not be Boltzmann suppressed. For GUT hadronic axions, this excludes the range $m_a \gtrsim 1$ eV.

We conclude that for $m_a = O(1\ \text{eV})$, axions cannot be firmly excluded by astrophysical considerations, so our proposed experiment is sensitive in one of the last remaining mass windows in which axions may exist. Conversely, if axions in this mass range were to be detected, the consequences for neutron star cooling, and SN dynamics would be very significant, apart from the paramount importance of such a discovery for particle physics.

1.5 Other axion experiments

An axion condensate would have formed in the early universe, and the universe would be

"overclosed" by axions[20] unless $f_a / N \lesssim 10^{12}$ GeV, i.e., $m_a \gtrsim 10^{-5}$ eV. Near saturation of this bound, axions would constitute the "cold dark matter" that is believed to dominate the universe. Axions clustered in our galaxy could be detected by their magnetic conversion into microwaves in a high-Q cavity[6]. An experiment of this sort is under way and has produced first negative results[21], but the sensitivity was two orders of magnitude less than needed to detect axions with a coupling to photons given by Eq. (3). Although this galactic axion search is of paramount importance for particle physics and cosmology, it is not clear at present whether the needed sensitivity can be reached in the near future.

Even for m_a of a few eV, thermally produced axions in the early universe would have survived in large numbers. Although their contribution to the cosmological mass density would be negligible, their present-day decay would be visible as a "glow" of the night sky[22]. Existing measurements of the brightness of the night sky exclude axion masses greater than a few eV .

Avignone *et al.*[23] have carried out an experimental search for double β decay using a high purity geramanium detector located underground. From the low energy portion of their spectrum ($E \leq 10$ keV), they were able to set limits on solar axions which would be detectable if they coupled to electrons (the axio-electric effect). However, the sensitivity of their detector was insufficient for the axion flux from the sun.

Another recently proposed experiment[24] addresses the magnetically induced bi-refringence of the vacuum, but would not be sufficiently sensitive[7] to detect axions which interact according to Eq. (3).

Our proposed experiment is the only laboratory method yet devised which is sensitive

enough to detect "invisible" axions. In the following sections we proceed to discuss details of our experimental design. In Section 2 we compute the axion flux expected from the sun. In Section 3 we calculate the axion-photon conversion efficiency rate in the presence of a medium, for arbitrary values of the real and imaginary parts of the photon dispersion relation. In Section 4 we discuss details of the detector design and background counting rates. A brief summary is given in Section 5.

2. The sun as an axion source

2.1 The axion spectrum

We confine our attention to hadronic axion models, where these particles do not interact with electrons at tree level. Such axions can be efficiently produced in the sun only by processes involving their coupling to photons given by Eq. (3). More generally, we consider (pseudo-) scalar particles which interact only by a two-photon vertex, for example, Sikivie's omions[10] and Anselm's arions[9,11]. In the interior of the sun, blackbody photons can convert into axions in the fluctuating electric fields of the charged particles in the plasma[25] (Fig. 1). The transition rate of a photon (actually a transverse plasmon) of energy ω into an axion is

$$R(\gamma \rightarrow a) = \frac{T\kappa^2}{(4\pi M)^2}\,\frac{\pi}{2}\left[\left(1+\frac{\kappa^2}{4\omega^2}\right)\ln\left(1+\frac{4\omega^2}{\kappa^2}\right)-1\right], \qquad (6)$$

where T is the temperature of the plasma. The Debye-Hueckel scale κ is given by

$$\kappa^2 = (4\pi\alpha/T)\sum_j Z_j^2 N_j\,, \tag{7}$$

where N_j is the number density of charged particles with charge $Z_j e$. The inverse of κ is the screening scale for charges in the plasma. The energy of the axion is close to the energy of the original photon; it is smeared over a narrow interval of width about equal to the plasma frequency[25]. Numerically, in the solar center, T = 1.3 keV, ω_p = 0.3 keV, and κ = 9 keV.

The axion luminosity of the sun is determined by folding the photon-axion transition rate from Eq. (6) with the blackbody photon distribution. The small spread of the axion energies for a given photon energy can be neglected. We integrate over a standard solar model[26] and find the differential axion flux plotted in Fig. 2 (solid line). Reasonable changes in the solar model would not change the axion luminosity significantly. The average axion energy is $\langle E_a \rangle$ = 4.2 keV.

The total axion luminosity (energy flux) is

$$L_a = 1.7 \times 10^{-3}\, L_\odot / M_{10}^2 = 3.6 \times 10^{-3}\, L_\odot\, (m_a/1\text{eV})^2 \tag{8}$$

where $L_\odot$ = 3.86 x 10^{33} erg sec^{-1} is the solar photon luminosity and $M_{10} = M/10^{10}$ GeV. Thus production of axions with 0.1 eV $\lesssim m_a \lesssim$ 5 eV would cause only a very minor perturbation of the sun.

We find that the differential axion spectrum at the earth is well approximated by

$$\Phi_a' \equiv d\Phi_a/dE_a = \frac{1}{M_{10}^2}\, 4.02\times10^{10}\,\mathrm{cm}^{-2}\,\mathrm{sec}^{-1}\,\mathrm{keV}^{-1}\,\frac{(E_a/\mathrm{keV})^3}{e^{E_a/1.08\mathrm{keV}}-1} \qquad (9)$$

where E_a is the axion energy — see the dashed line in Fig. 2. The total axion flux at the earth is

$$\Phi_a = 3.54 \times 10^{11}\ \mathrm{cm}^{-2}\ \mathrm{sec}^{-1}\ (M_{10})^{-2} = 7.44 \times 10^{11}\ \mathrm{cm}^{-2}\,\mathrm{sec}^{-1}\ (m_a/1\mathrm{eV})^2 \qquad (10)$$

2.2 Size of the solar axion source

The radial distribution of the axion energy loss rate, dL_a/dr shown in Fig. 3, is based on the standard solar model of Ref. 26. Most axions emerge from a region within 0.2 $R_\odot$ (radius of the solar disk). The average distance between the sun and the earth is 215 $R_\odot$. Thus the angular radius of the axion source region as viewed from the earth is $\delta_a \approx (0.2/215) = 0.9\times10^{-3}$ radian. This is important if one were to include an x-ray collimator in the experimental setup.

3. Axion-photon conversion rate

3.1. Equation of motion

We now proceed to calculate the axion-photon conversion rate in the presence of a nearly homogeneous magnetic field **B** and a refractive medium. From very general arguments[7] one finds that only the photon component with polarization (electric field) parallel to the magnetic field mixes with axions. By "parallel" component we mean the polarization state whose electric field vector lies in the plane of the wave vector **k** and the magnetic field **B**. The photon electric field is parallel to **B** only if the propagation is strictly transverse to the magnetic field. Denoting the amplitude of this parallel photon component by A and the amplitude of the axion field by a, the relevant wave

equation is[7]

$$i\partial_z \begin{pmatrix} A \\ a \end{pmatrix} = \begin{pmatrix} \omega - m_\gamma^2/2\omega - i\Gamma/2 & B/2M \\ B/2M & \omega - m_a^2/2\omega \end{pmatrix} \begin{pmatrix} A \\ a \end{pmatrix} \qquad (11)$$

with B the component of **B** transverse to the wave vector **k**, and M is defined by Eq. (3). The photon refractive index has been written, without loss of generality, $n_\gamma = 1 - m_\gamma^2/2\omega^2 - i\ \Gamma/2\omega$ where in general, m_γ and Γ are functions of ω and z. Γ is the damping coefficient, or inverse absorption length for the x-rays. The quantities m_γ and Γ are easily related to the usual atomic scattering factors f_1 and f_2 as tabulated, e.g., by Henke *et al.*[27]. We have completely neglected the imaginary part of the *axion* refractive index because of the extremely weak axion interaction strength. We stress that the linearized form Eq. (11) of the Klein-Gordon equation is applicable only in the limit of small refractive effects, i.e., when $\omega >> m_a^2/2\omega$ and $\omega >> |m_\gamma^2/2\omega + i\Gamma/2|$.

3.2 An upper limit to the expected x-ray flux

An absolute ceiling can be placed on the axion-photon conversion that can be achieved with a given field strength and a given path length. If the diagonal entries of the mixing matrix Eq. (11) are taken to be real and equal, and assuming a homogeneous field and starting with a pure axion beam, one finds that after a distance L the probability of measuring a photon is given as

$$p_\gamma(L) = (B/2M)^2\, L^2 \qquad (12)$$

This approximate result holds only if $p_\gamma << 1$. For B = 3 Tesla and $M = 1\times10^{10}$ GeV we find $B/2M = 1.48\times10^{-12}\ \mathrm{cm}^{-1}$, so that for path lengths in the meter range this condition is well-satisfied. All effects which occur from the non-equality of the diagonal entries in the mixing matrix or from

the imaginary parts will reduce this result. From Eq. (10) and Eq. (12), an absolute ceiling to the expected x-ray flux in the detector from solar axion conversion is

$$\Phi_{max} = \Phi_a \times p_\gamma(L) = 5.3 \times 10^{-7}\ \mathrm{cm}^{-2}\ \mathrm{sec}^{-1}\ (B/3\mathrm{T})^2\ (L/400\mathrm{cm})^2\ (m_a/1\ \mathrm{eV})^4 \qquad (13)$$

This result sets an upper limit to the magnitude of the x-ray flux from axion conversion which we may attempt to detect.

3.3 General result for the transition rate

In general, the dispersion relations for axions and photons are not identical. Therefore we need to determine a general solution to the "Schroedinger equation" Eq. (11). To this end we make use of the "perturbed wavefunction" approach outlined in Ref. 7. Note, however, that the "Hamiltonian" in Eq. (11) is not Hermitian so that one has to modify the procedure to solve this equation accordingly. From a first order perturbative solution we find for the transition *amplitude*, aside from an overall phase,

$$\begin{aligned} \langle A(z)|a(0)\rangle = (1/2M)\ \exp\Big\{-\int_0^z dz'\Gamma/2\Big\} \times \\ \times \int_0^z dz' B\ \exp\Big\{i\int_0^{z'} dz''\Big[(m_\gamma^2 - m_a^2)/2\omega - i\Gamma/2)\Big]\Big\}. \end{aligned} \qquad (14)$$

This result is first order in the small quantity $Bz/2M$, but completely general otherwise. Note that in general B, Γ, and m_γ are functions of z. We now consider the case where the matter density within the detector is uniform so that m_γ and Γ are constant, and we also take **B** to be uniform. Also, we use

$$q = |(m_\gamma^2 - m_a^2)/2\omega| \tag{15}$$

for the momentum difference between photons in the medium and axions. Then we find for the probability of observing a photon at $z = L$

$$p_\gamma(L) = \frac{(B/2M)^2}{q^2 + \Gamma^2/4}\left[1 + e^{-\Gamma L} - 2e^{-\Gamma L/2}\cos(qL)\right]. \tag{16}$$

In the absence of damping ($\Gamma = 0$) this is the usual result for the transition between two mixed particle states and $2\pi/q$ can be interpreted as the oscillation length ℓ_{osc}. In the limit $q \to 0$ and $\Gamma \to 0$ we recover Eq. (12).

Using a buffer gas which absorbs x-rays by the photoelectric effect (non-zero damping Γ), one could measure all of the photons produced along the axion path, by collecting and counting the photo-electrons. The probability that an axion is absorbed in just the probability that it is neither in an axion nor in a photon state at $z = L$, i.e. $p_{abs}(L) = 1 - p_a(L) - p_\gamma(L)$. The probability $p_a(L)$ that an axion is still in the beam at $z = L$ is determined from a second order solution of the perturbed wave function method. Assuming uniformity of B, m and Γ we find

$$p_{abs} = \frac{(B/2M)^2}{(q^2 + \Gamma^2/4)^2}\left\{q^2 - 3\Gamma^2/4 + \left(q^2 + \Gamma^2/4\right)\left(\Gamma L - e^{-\Gamma L}\right)\right. \tag{17}$$
$$\left. + \left[\Gamma^2\cos(qL) - 2q\Gamma\sin(qL)\right]e^{-\Gamma L/2}\right\}.$$

This result is mainly of interest for strong photon absorption, i.e., for $\Gamma L >> 1$. Then we find the simple approximation

$$p_{abs} = \frac{(B/2M)^2}{q^2 + \Gamma^2/4}\,\Gamma L \tag{18}$$

The maximum rate occurs for $\Gamma = 2q$. In this case the absorption probability is $p_{abs} = (B/2M)^2\, 2L/\ell$, which is smaller than the optimum value of $P\gamma(L)$ for the dispersion-matching scheme [given in Eq. (12)] by the factor $2\ell/L$, where $\ell \equiv \Gamma^{-1}$ is the absorption length. This result could have been anticipated, aside from numerical factors, on the basis of Eq. (12): it is advantageous to absorb the photon component within an oscillation length, i. e. $\ell \lesssim 1/q$, because for larger distances one does not gain any further strength of the photon component. For about a distance ℓ one may apply Eq. (12), after which the photon gets absorbed and one starts again with a pure axion beam. There are about L/ℓ such steps, giving this simple result within a factor of two.

Although $p_{abs}(L)$ is smaller than $p_\gamma(L)$, the axion mass sensitivity region Δ is wider in the absorption detector, so that the time required to search a given mass region would be about the same in the absence of background. (But not with background present, see Section 4.2). The broadband detector may be useful to detect axions with mass above a few eV, since high pressure gas containment is not needed.

4. Practical Detector Design

4.1. Design Concept

We conceive that the most practical implementation of an axion helioscope would be designed to fit in a stationary, large-volume high-field superconducting magnet. To discuss the response of this detector concretely, we will assume a solenoidal magnet of nominal (but demonstrated [28])

dimensions and field: diameter D = 4 m, length S = 3 m and average field B = 3 T. A vessel containing the buffer gas (H_2 or He) of variable pressure would be placed within the magnet bore. The inside *surface* of the vessel would be instrumented all around with appropriate x-ray detectors (see Fig. 4). The detector might be, for example, a thin cylindrical multiwire chamber with a conventional proportional gas (Ne, Ar or Xe) separated from the dispersion gas by a thin window[29]. The magnet axis would be oriented north-south, so that the magnetic field is roughly perpendicular to the axion flux (i. e. sun) at all times.

4.2. Rates and Values

In this section we use the formalism of Section 3 to derive operating values for a realistic device and the corresponding range of sensitivity to axion mass and axion photon coupling (m_a, M). The plasma frequency (effective mass) for an x-ray in a gas can be expressed in terms of f_1, the real part of the atomic scattering factor[27] as

$$\omega_p^2 \equiv m_\gamma^2 = 4\pi r_0 (N_A/A\, m_u)\, \rho f_1 \qquad (19)$$

where r_0 is the classical electron radius, N_A is Avogadro's number, A is the atomic mass number of the gas, m_u is the atomic mass unit, and ρ is the gas density. The use of a gas with the lowest possible Z is clearly indicated for two reasons. First, the real part of the atomic scattering factor f_1 is linear in Z, whereas the absorptive part (proportional to the mass attenuation coefficient) increases roughly as Z^3. Second, because the ionization energies of H_2 and He are very low, the variation of $f_1(\omega)$ in the relevant range ω = (1-10) keV is sufficiently weak that the matching of the dispersion relations can be achieved *simultaneously* over this entire range of energies. For these gases, the asymptotic value $f_1(\omega \rightarrow \infty) = Z$ is taken on with sufficient

precision over our entire range of interest. Eq. (19) implies an operating pressure (at 300 K) of P = 14.83 $(m_\gamma/1\ \mathrm{eV})^2$ atm, where m_γ is the chosen photon mass. The pressure is the same for both H_2 and He because H_2 is diatomic. Searching from 0.1 eV to 5 eV in axion mass dictates a large pressure range going from roughly 0.1 to 340 atm. Operation at liquid nitrogen temperature (77 K) would reduce the *pressure* by roughly a factor of 4 for the same *density*. Absorption of the x-rays is not significant, even for a search mass as high as 5 eV.

For a given mass of the axion, the total rate of appearance of x-rays in a detector with cross-section A and over the whole axion spectrum is given by

$$R = \int \mathrm{ds} \int \mathrm{dy} \int \mathrm{d}E_a \, \Phi_a' \, p_\gamma[L(y)] \, . \qquad (20)$$

Here Φ_a' is the differential solar axion flux as given by Eq. (9), and $L(y)$ is the path length through the detector volume at a given transverse position y. The conversion probability $p_\gamma[L(y)]$ depends on the axion-photon coupling strength, and implicitly on both m_a and E_a through q of Eq. (16). In Eq. (20) we have assumed that the axions traverse the chamber perpendicular to the magnetic field. As discussed later, this implies no great loss of generality.

At a fixed pressure P (hence search mass m_γ), the response of the detector will be a sharply peaked function of the actual axion mass m_a. In Fig. 5 we show the x-ray production rate integrated over energy and detector area as a function of m_a, where the pressure has been set to m_γ = 1.000 eV. The GUT value of E/N = 8/3 has been assumed. The *width* of the response curve scales as m_γ^{-2}, with the fractional full-width half-maximum $\Delta \equiv |m_p - m_a|/m_\gamma \approx 1.2 \times 10^{-3}$ $(m_\gamma$ /1 eV$)^{-2}$ for L = 4 meters. An alternative magnet with higher field and smaller bore D, could be advantageous, since the fractional mass bandwidth varies inversely with L, and $L \approx$ D. If axions

were found to exist, the resulting x-ray spectrum would faithfully reproduce the axion spectrum since $\omega = E_a$ (Fig. 2), aside from absorptive effects, and assuming the response curve is optimized by gas density, i.e., $m_\gamma = m_a$. If the gas density were set substantially off the maximum of the response curve, the measured spectra and distribution in transverse position y would be modulated non-trivially as the oscillation length $\ell_{osc}(m_a, E_a, P)$ becomes comparable to $L(y)$. The overall rate expected, again for GUT and assuming $m_\gamma = m_a$, is shown in Fig. 6. The rate varies essentially as m_a^4, since the solar axion emission and the detector sensitivity each contribute factors of m_a^2. The slight deviations from m_a^4 behavior is the result of the (small) absorption in the H_2 and He buffer gas.

The alternative scheme, using an x-ray absorbing gas mixture, has two advantages when used to search for axions near the high mass end of the range. (1) High gas pressures are not needed since Γ can be increased several orders of magnitude by using a mixture of helium and a high Z gas. (2) Scanning of gas pressure is unnecessary since the detector is sensitive to axions with a wide range of m_a without adjustment.

For this alternative scheme we would choose a gas mixture which contains a heavy gas whose K absorption edge lies near or somewhat below the expected x-ray energy. As previously shown, the optimal transition rate will occur for $\Gamma = 2q = m_a^2/E_a$. Thus for a chosen value of Γ the optimal rate occurs for $m_a = m_\Gamma \equiv (\Gamma E_a)^{1/2}$. In fact, we can optimize Γ as a function of energy i.e. $\Gamma \propto 1/E_a$, by selecting a suitable mixture of gases such as 70% neon and 30% argon; with K absorption edge energies of ~1 keV and ~3.2 keV respectively.

The total x-ray rate is given by Eq. (20) with $p_{abs}(L)$ substituted for $p_\gamma(L)$. As a simplifying approximation, we take $E_a = 4.2$ keV, the mean energy of the solar axions. Then the

expected count rate

$$R_{abs} = \Phi_a \times p_{abs} \times V = 1.3 \times 10^{-7}\,\mathrm{sec}^{-1}\,(B/1\mathrm{T})^2\,(V/1\mathrm{m}^3)\,m_\Gamma^2\,m_a^4/(m_\Gamma^4 + m_a^4), \qquad (21)$$

where m_Γ and m_a are in units of eV. The x-ray rates in the nominal detector are shown in Fig. 7 for several values of Γ. Also shown is the envelope curve which results from re-optimizing Γ at each value of m_a. This curve is also plotted in Fig. 6 for comparison. Although the x-ray rate is smaller than in the first scheme by $\sim 10^4$, the axion mass sensitivity region Δ is wider by the same factor, so that in the absence of background, the time required to search a given mass region and detect the same number of x-rays from axion conversion would be about the same. In the presence of background, however, the tuned detector is more sensitive, since the axion signal counts will all appear at one gas pressure and give a higher count rate. Furthermore, in the broad-band scheme, the total mass of sensitive gas is very much greater than in the tuned detector scheme, and so the background due to natural or cosmogenic radioactivity would be proportionately greater.

4.3. Limits of Applicability

It is of interest to know over what range of axion mass m_a (or more fundamentally what range of f_a/N) this experiment will be sufficiently sensitive to detect axions if they have the standard coupling. However, we emphasize that from an experimental viewpoint, such an experiment really addresses a region in the two-dimensional parameter space of axion mass *and* axion-photon coupling (m_a, M).

In this detector design (exact matching of the photon and axion masses), measurement is possible, in principle, down to exactly massless Goldstone bosons, if the axion-photon coupling is

sufficiently strong (non-standard). The upper limit of the accessible mass range is somewhat arbitrary, and would depend largely on engineering considerations (containment of high pressure gas). An axion mass of 5 eV is a reasonable upper limit without undue complications; larger axion masses are accessible using the alternate scheme.

The limiting value of axion-photon coupling for which axion detection is possible depends on the background. For a device of dimensions and field specified above a reasonable goal would appear to be $M \approx 10^{11}$ GeV, corresponding to a lower mass limit of $m_a \approx 0.1$ eV for standard axion-photon coupling. This implies a background photo-electron rate significantly below 10^{-5} sec^{-1} (see Fig. 6). Clearly such an experiment would have to be conducted underground for adequate suppression of cosmic rays. We argue that the other (and generally more problematic) source of background, namely natural and cosmogenic activities from the environment and construction material could be kept to that level. These are mostly gammas and x-rays. The argument is based on a rather straightforward scaling of the low-energy spectra (<10 keV) seen in state-of-the-art germanium detector $\beta\beta$ experiments. Attention has been paid to this end of the spectra recently in setting limits on cold dark matter. For one such 0.7 kg Ge detector (PNL/USC), the total background over the range 4 keV < E < 10 keV is already bounded at 3×10^{-5} counts keV^{-1} day^{-1}, and a factor of ten reduction is forthcoming with only minor improvements[30]. We take the active detection region of the present experiment to consist of Xe proportional gas of one attenuation depth for 4 keV photons (≈0.1 mg/cm^2), over the entire inside rear surface of the bore. Then the total active detector mass would be ≈170 g. The incoherent Compton cross section $\sigma_C \propto Z \propto A$, so scaling to the total active detector mass gives us the desired result, when integrated over a 10 keV interval encompassing the axion spectrum (Figure 2). Of course, this implies that all of the care taken in material selection for construction and shielding in the $\beta\beta$ experiments must be taken rigorously in the present case, in an extended rather than compact

geometry.

We emphasize that the required background rate is very sensitive to the axion mass search range. Since the expected axion-photon conversion rate $\propto m_a^4$, a background 10^2 greater than estimated above still will permit a search down to $m_a \approx 0.3$ eV, as shown in the following section. At this value of m_a, the required H_2 or He gas pressure $P \approx 1.335$ atm at 300 K.

4.4. Counting Time vs. Background

This experiment is a *tuning* experiment in which the density of the dispersion matching gas is varied, in order to enhance the conversion probability of the axion into an x-ray within a narrow window of axion mass. A detailed strategy of optimization is not in order here, but a simple estimate of counting time follows.

The fractional full-width half-maximum Δ of the response curve has the approximate value $\Delta(m\gamma) \approx 10^{-3}(m\gamma/\mathrm{eV})^{-2}$. The number N of discrete steps in gas density that must be taken to search a range of axion masses (m_1, m_2) is

$$N = \int_{m_1}^{m_2} \frac{dm}{m\,\Delta(m)} \approx 500\ (m_2^2 - m_1^2)/(1\ \mathrm{eV})^2 \approx 500\ (m_2/1\mathrm{eV})^2. \qquad (22)$$

To establish a uniform limit in M throughout the mass range, equal time would be devoted to each mass bin to achieve the desired confidence level. Due to the proliferation of bins as m_2 increases, m_2 determines the required search time in this case. The search is therefore able to set a uniform limit on M for a broad range of m_a, without tying the measurement to any particular

axion model.

On the other hand, simply to exclude GUT axions over the same window considerably shortens the search time. The overall counting rate is $R(m_a) \approx 3 \times 10^{-2}$ sec^{-1} $(m_a/1\ \text{eV})^4$ $(B/3\text{T})^2$ (S/3m) $(D/4\text{m})^3$. The required search time is

$$t \propto \int_{m_1}^{m_2} \frac{dm}{m\,\Delta(m)\,R(m)}, \tag{23}$$

and for the detector described in Section 4.1 we find, if each bin is observed for a time sufficient to detect one signal count if m_a lies in that bin,

$$t = 1.6 \times 10^6 \text{sec}\ [(1\ \text{eV}/m_1)^2 - (1\ \text{eV}/m_2)^2] \approx 1.6 \times 10^6\ \text{sec}\ (1\ \text{eV}/m_1)^2. \tag{24}$$

Due to the increased counting time for lower masses, m_1 determines the time in this case.

We denote the conversion (signal) rate corresponding to the desired bound on M by $R_s \equiv (M_{lim})$ then, $\tau\ (\equiv R_s^{-1})$ is the time required to see, on the average, 1 signal event. For $M_{lim} = 5 \times 10^{10}$ GeV, $\tau = 1$ day in the present case. The background rate, denoted by R_b, is assumed to be distributed in a purely statistical manner.

The presence of background counts during the search for axions has two consequences. First, an upward fluctuation in background rate can mimic an axion signal, giving a "false alarm". This is not a serious problem in this experiment, since the detector can be retuned to only those bins which gave apparent signals to re-check the rate with better statistics. Second, a downward

fluctuation in background can conceal a real axion signal, and this reduces the confidence level of a null result. But if an axion signal is twice as large as the downward fluctuation in background, it will be detected. Then it can be confirmed by re-measurement as stated above.

We distinguish three cases:

(i) $R_b << R_s$. If the background is much smaller than the expected signal, and assuming that axions do not exist in the mass bin being measured, the usual outcome will be to measure *no* events (signal or background) in τ or several τ. Thus the limit M_{lim} is established at the 90% confidence level (C. L.) after counting for a time $t = 2.3\,\tau$.

(ii) $R_b \approx R_s$. If the background is comparable to the signal rate at M_{lim}, but again assuming that axions in fact do *not* exist within the mass bin being measured, then *on the average* in a counting interval 4τ, one will observe 4 events (background). Then, one can exclude, again at the 90% C. L., a signal contribution of twice this magnitude, i.e. corresponding to $M = M_{lim}/2^{1/4} = 4.2\times10^{10}$ GeV. As already discussed, the factor of 2 in rates rules out a false negative result caused by a downward fluctuation of background coinciding with an actual axion signal.

(iii) $R_b >> R_s$. Here if τ is already a significant time, the time required to place a bound on M_{lim} over a broad range of m_a would be prohibitive. However, the limit on M which can feasibly be established falls only slowly with increased background rate. For example, if $R_b = 100$ day^{-1} on the average, then in one day we will observe 100 ± 16 counts (90% C.L.) for the nominal detector described in this paper. Since the count rate varies as M^{-4}, we are able to exclude $M < 2 \times 10^{10}$ GeV which is only a factor of two worse than the limit on M which can be set if $R_b = 1$ day^{-1}.

4.5 Operational Considerations

It should be noted that the fractional mass bandwidth Δ of the detector narrows rapidly with increasing mass. This dictates that the density of the dispersion gas must be uniform to $(\Delta n/n) << 2\Delta$ for the response curve to be determined by the oscillation length, and not washed out. For $m_a \approx 5$ eV, this implies, among other things, that the temperature differential must be held to $\sim 6 \times 10^{-3}$ K at 77 K. *A fortiori*, the monitoring and reproducibility of the density must be as stringent. Note that the gravitational density gradient is not a significant problem even at the highest end of the mass range. At $m_a = 5$ eV, to keep the response curve sharp, we require $\Delta n/n < 10^{-4}$. Even in the less favorable case of He as a dispersion-matching gas (A = 4), the fractional density difference for a 4 m difference in height would be $\sim 7 \times 10^{-5}$.

The optimum direction of the magnet axis and B is perpendicular to the direction of the sun. If the magnet axis is aligned in a north-south direction, the orientation of the detector with respect to the sun will vary somewhat as the earth rotates, but the detector will remain sensitive. For a long solenoid no penalty is incurred for moderate misalignment angle θ. This surprising result follows from eq. (12), where the detection rate $R \propto B^2L^2$. While the useful component of the field $B_\perp = B \cos\theta$, the path length in the detector increases to $L = D/\cos\theta$, which compensates. An alternative design would employ a short magnet with its axis aligned east-west, then the axion $\rightarrow$ x-ray $\rightarrow$ photoelectron counting rate would be strongly modulated with a 12 hour period, which could be useful in separating the solar axion signal from background.

5. Summary

The construction and operation of an axion helioscope appears to be a practical possibility,

and would substantially extend our knowledge about the realization of the Peccei-Quinn mechanism in nature. The uncertainties of the astrophysical bounds, in conjunction with the freedom of the relevant parameters of the axion models, appear to be sufficiently severe to warrant an independent experimental effort. It is remarkable that our search would be most sensitive in a regime just between the ranges excluded by two very different astrophysical arguments, which may not overlap. A detection of axions in this range, aside from its paramount importance for particle physics, would be of great importance for astrophysics. A negative search result would definitively close one of the two remaining axion mass windows.

We acknowledge useful discussions with J. Bjorken, A. Kerman, H. Nelson, R. Peccei, B. Schumacher and L. Stodolsky. We thank P. J. Oddone and R. A. Muller for their encouragement. This work was performed under the auspices of the U.S. Department of Energy under contract numbersW-7405-ENG-48 (LLNL), DE-AS05-81ER40039 (Texas A&M), DE-FG03-84ER-40161 (UC-Berkeley), DE-AC03-76SF00098 (LBL) and by the National Aeronautics and Space Administration under contract number NGR05-003-578.

REFERENCES

1. R.D. Peccei, H. R. Quinn, *Phys. Rev. Lett.* **38**, 1440 (1977) and *Phys. Rev.* **D 16**, 1791 (1977).
2. S. Weinberg, *Phys. Rev. Lett.* **40**, 223 (1978); F. Wilczek, *Phys. Rev. Lett.* **40**, 279 (1978).
3. For reviews see J.E. Kim, *Phys Rep.* **150**, 1 (1987); H.-Y. Cheng, *Phys, Rep.* **158**, 1 (1988).
4. D.B. Kaplan, *Nucl. Phys.* **B 260**, 215 (1985).
5. M. Srednicki, *Nucl. Phys.* **B 260**, 689 (1985).
6. P. Sikivie, *Phys. Rev. Lett.* **51**, 1415 (1983); (E) *ibid.* **52**, 695 (1984).
7. G. Raffelt, L. Stodolsky, *Phys. Rev.* **D 37**, 1237 (1988).
8. D. E. Morris, Lawrence Berkeley Laboratory Report LBL-19594 (May 1985) and unpublished work; K.van Bibber, G.G. Raffelt, D. M. Moltz, F. R. Huson, J. T. White, P. M. McIntyre, R. N. Boyd, H. N. Nelson, *Fermilab Letter of Intent*, P-794 (March 1988).
9. A. A. Anselm, *Phys. Rev.* **D 37**, 2001 (1988). When considering the effect of conversion in a medium with $n \neq 1$, Anselm neglected the important case where $n < 1$ which is relevant for keV x-rays in a low–Z gas. Thus, he incorrectly concluded that the detection of solar axions was not feasible.
10. P. Sikivie, *Phys. Rev. Lett.* **61**, 783 (1988).
11. A. A. Anselm and N. G. Uralsev, *Phys. Lett.* **114 B**, 39 (1982).
12. G. Raffelt, D. Dearborn, *Phys. Rev.* **D 36**, 2211 (1987).
13. N. Iwamoto, *Phys. Rev. Lett.* **53**, 1198 (1984).
14. S. Tsuruta, K. Nomoto, 1986, IAU-Symposium No. 24, *Observational Cosmology*, in press.

15. D. E. Morris, *Phys. Rev.* **D 34**, 843 (1986).

16. G. Raffelt, D. Seckel, *Phys. Rev. Lett.* **60**, 1793 (1988); M. Turner, *Phys. Rev. Lett.* **60**, 1797 (1988); R. Mayle et al., *Phys. Lett.* **203 B**, 188 (1988).

17. G. G. Raffelt, *Phys. Lett.* **166 B**, 402 (1986).

18. D.S.P. Dearborn, D.N. Schramm, G. Steigman, *Phys. Rev. Lett.* **56**, 26 (1986).

19. R. F. Harndon et al., *Bull. Am. Astron. Soc.* **11**, 424 (1979) and *Bull. Am. Astron. Soc.* **11**, 789 (1979).

20. J. Preskill, M. B. Wise, F. Wilczek, *Phys. Lett.* **120 B**, 127 (1983); L. F. Abbott, P. Sikivie, Phys. Lett. **120 B**, 133 (1983); M. Dine, W Fischler, *Phys. Lett.* **120 B**, 137 (1983).

21. S. DePanfilis, *et al.*, *Phys. Rev. Lett.* **59**, 839 (1987).

22. T. W. Kephart, T. J. Weiler, *Phys. Rev. Lett.* **58**, 171 (1987); M. S. Turner, *Phys. Rev. Lett.* **59**, 2489 (1987).

23. F. T. Avignone III, R. L. Brodzinski, S. Dimopoulos, G. D. Starkman, A.K. Drukier, D. N. Spergel, G. Gelmini, B. W. Lynn, *Phys. Rev.* **D 35**, 2752 (1987): S.P. Ahlen, F. T. Avignone III, R. L. Brodzinski, A. K. Drukier, G. Gelmini, D. N. Spergel, *Phys. Lett.* **B 195**, 603 (1987).

24. L. Maiani, R. Petronzio, E. Zavattini, *Phys. Lett.* **175 B**, 359 (1986); A.C. Melissinos, *et al*, Brookhaven Experimental Proposal E-840, 1987 (approved).

25. G. Raffelt, *Phys. Rev.* **D 37**, 1356 (1988).

26. J. Bahcall *et al.*, *Rev. Mod. Phys.* **54**, 767 (1982).

27. B.L. Henke *et al.*, *Atomic Data and Nuclear Data Tables* **27**, 1 (1982).

28. For example, the FNAL 15 ft. bubble chamber magnet.

29. U. Gastaldi, *Nucl. Instr. and Meth.* **156**, 257 (1978). The application was the study of $p\bar{p}$ atomic x-rays and thus was precisely for the same range of energies as ours, 1–15 keV.

Furthermore, the construction and operation of this chamber was the same as envisioned, it had variable pressure H_2 on the inside, and a cylindrical multiwire chamber filled by higher-Z gas of the same pressure on the outside.

30. F.T. Avignone III, R.L. Brodzinski, Pacific Northwest Laboratory preprint PNL-SA-15497 (December, 1987); and R.L. Brodzinski, *private communication* .

FIGURE CAPTIONS

Figure 1

Feynman diagram for the Primakoff production of axions by the interaction of a photon with an electron or nucleus (top), and (bottom) axion-photon conversion in the electric or magnetic field of an external source denoted by a cross (×).

Figure 2

Differential solar axion flux at the earth. We assume that axions are only produced by the Primakoff conversion of blackbody photons in the solar interior ("hadronic axions"), and we assume a standard solar model[26]. The axion-photon coupling strength M is defined in Eq. (3). The solid line arises from a numerical integration over the sun, the dashed line is an analytical approximation to this result as given in Eq. (9).

Figure 3

Radial distribution of the axion energy loss rate of the sun. The radial coordinate r is in units of the solar radius $R_\odot$.

Figure 4

Schematic design of the detector employing a multiple wire proportional chamber (MWPC).

Figure 5

Conversion rate as a function of m_a for the detector shown in Fig. 4, with D = 4m, S = 3m and B = 3 Tesla. The dispersion gas density is chosen such that m_γ = 1.000 eV, and thus is optimized

for conversion of axions with $m_a = 1.000$ eV. The dashed line is a blow-up of the solid line; the corresponding scale is on the upper horizontal axis.

Figure 6

Total rate of axion-photon conversion in the dispersion matching detector as a function of the axion mass m_a. As in Fig. 5, the relationship between m_a and the axion-photon coupling M is given by Eq. (4) and the GUT value $E/N = 8/3$ is used. The density of the dispersion gas is assumed to be re-adjusted to the optimal value for each value of m_a. At the largest values of m_a, corresponding to the highest gas densities, the rate with He as a dispersion gas (dashed line) is lower than that for H_2 (solid line) because of the increased importance of absorption in the higher-Z medium. The dash-dot line indicates the conversion rate in an absorption gas detector with $m_a = m_\Gamma$ for comparison. Although the sensitivity is much lower, it is sensitive to a wide range of axion masses simultaneously.

Figure 7

Total rate of axion-photon conversion in the absorption type detector: (dotted line) gas mixture and pressure chosen to maximize the count rate for $m_a \approx 1$eV, (dashed line) optimized for $m_a \approx 10$ eV, (dotted-dashed line) for $m_a \approx 100$ eV, (solid line) the envelope curve for $m_a \approx m_\Gamma$, also plotted in Fig. (6).

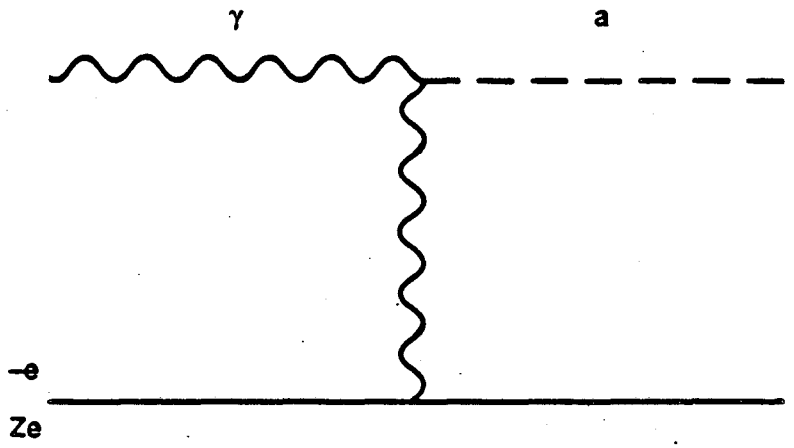

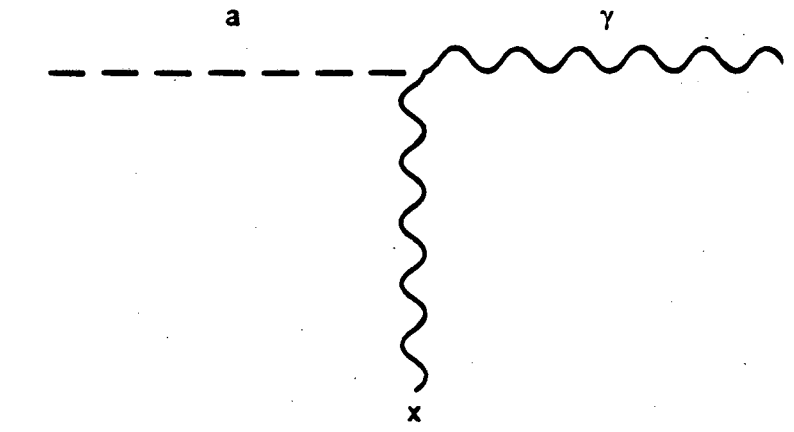

Figure 1

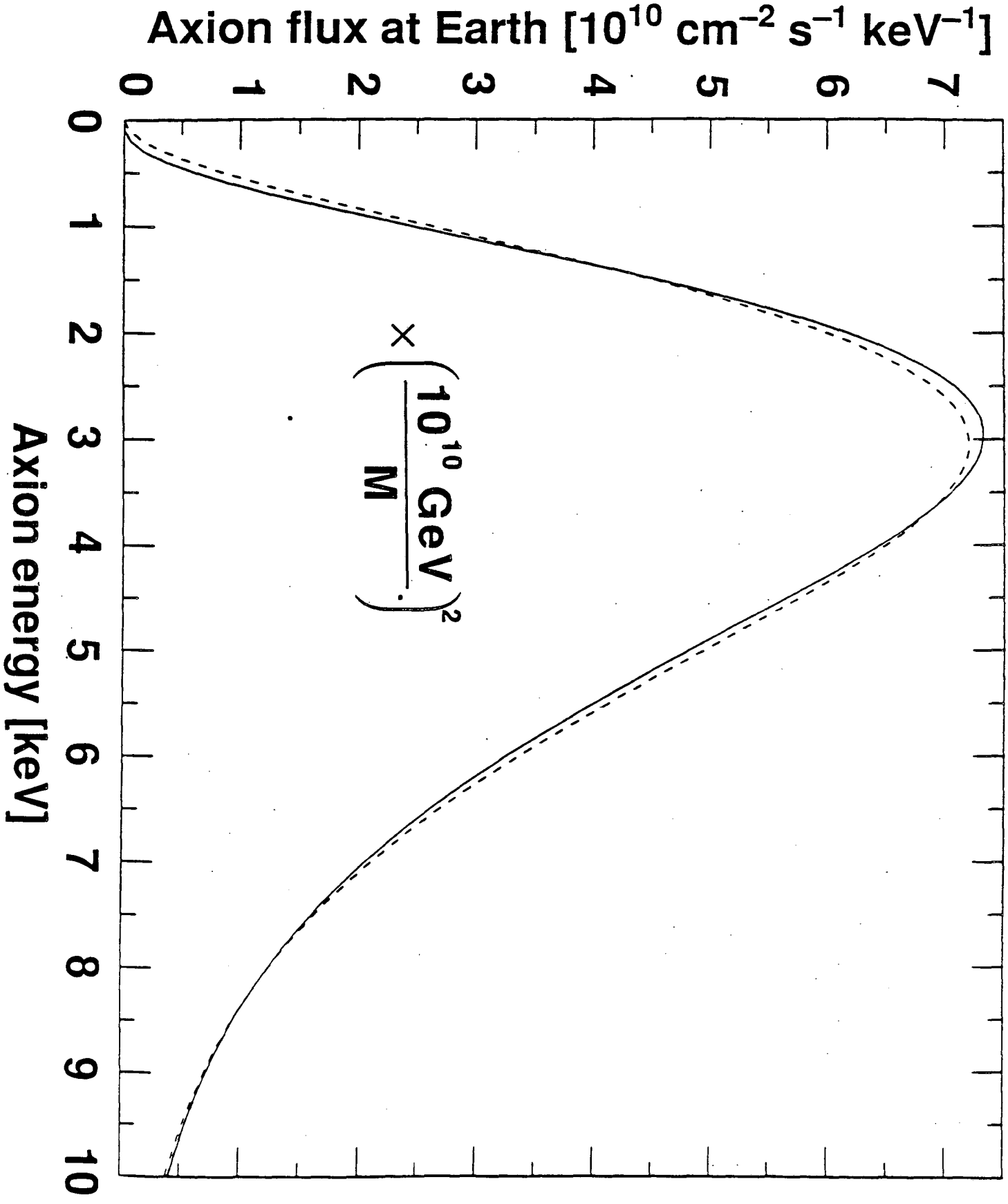
Axion flux at Earth [10^{10} cm^{-2} s^{-1} keV^{-1}]
0 1 2 3 4 5 6 7
Axion energy [keV]
0 1 2 3 4 5 6 7 8 9 10
$\times \left(\frac{10^{10}\ \text{GeV}}{M}\right)^2$

Figure 2

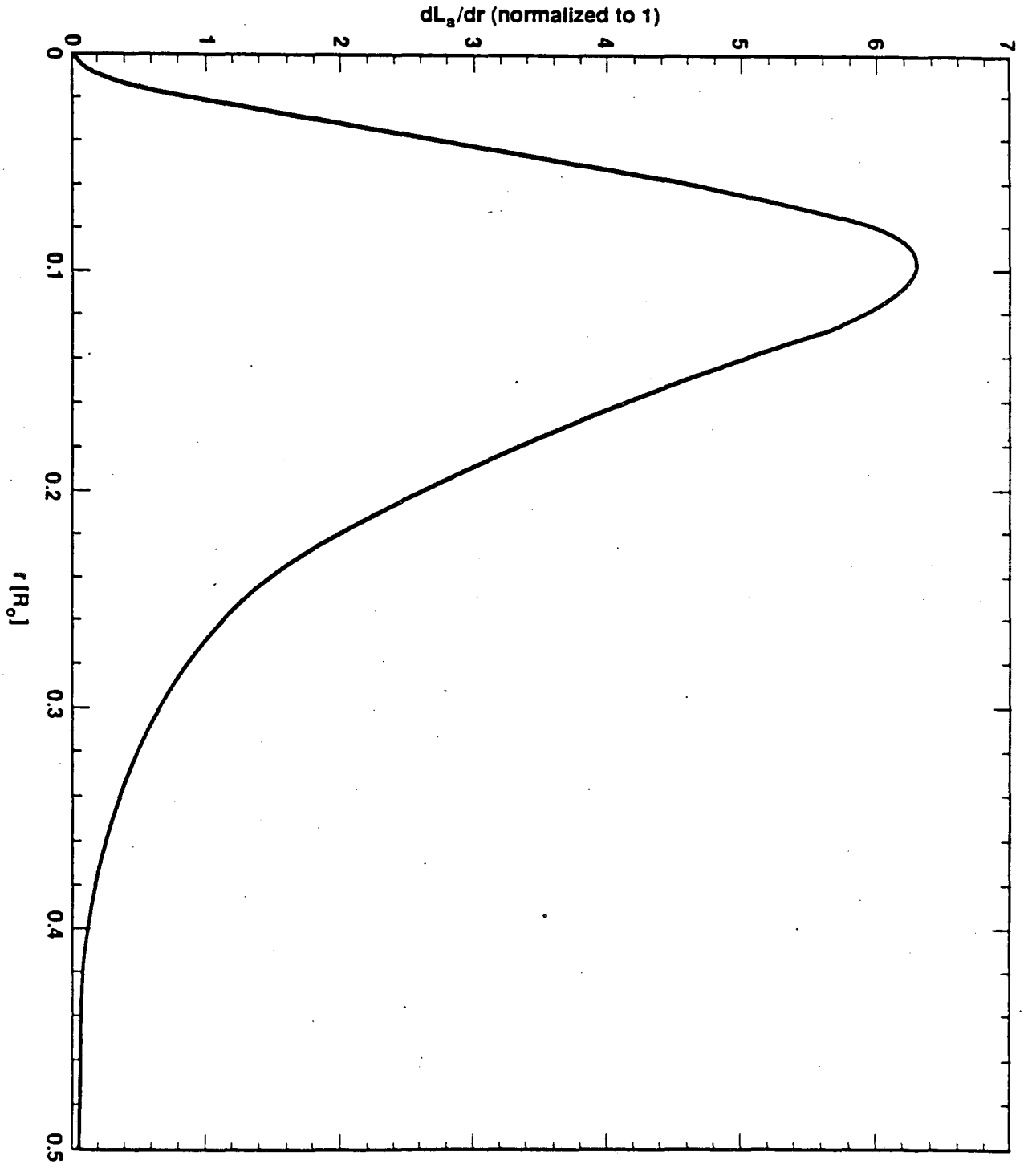
AH-118-U-5704-3
dL$_s$/dr (normalized to 1)
0
1
2
3
4
5
6
7
0
0.1
0.2
0.3
0.4
0.5
r [R$_o$]

Figure 3

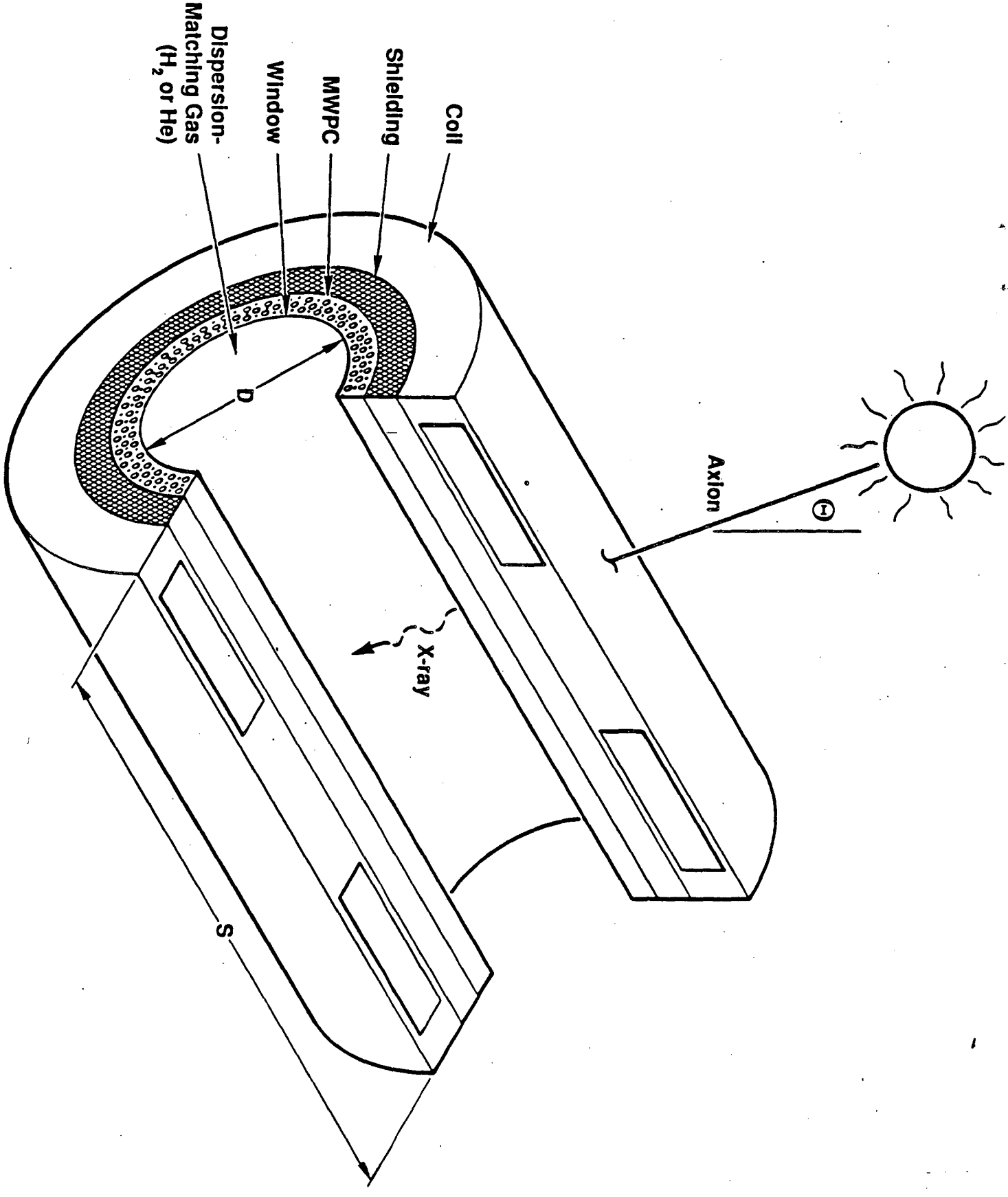
Dispersion-
Matching Gas
(H_2 or He)
Window
MWPC
Shielding
Coil
D
S
X-ray
Axion
θ

Figure 4

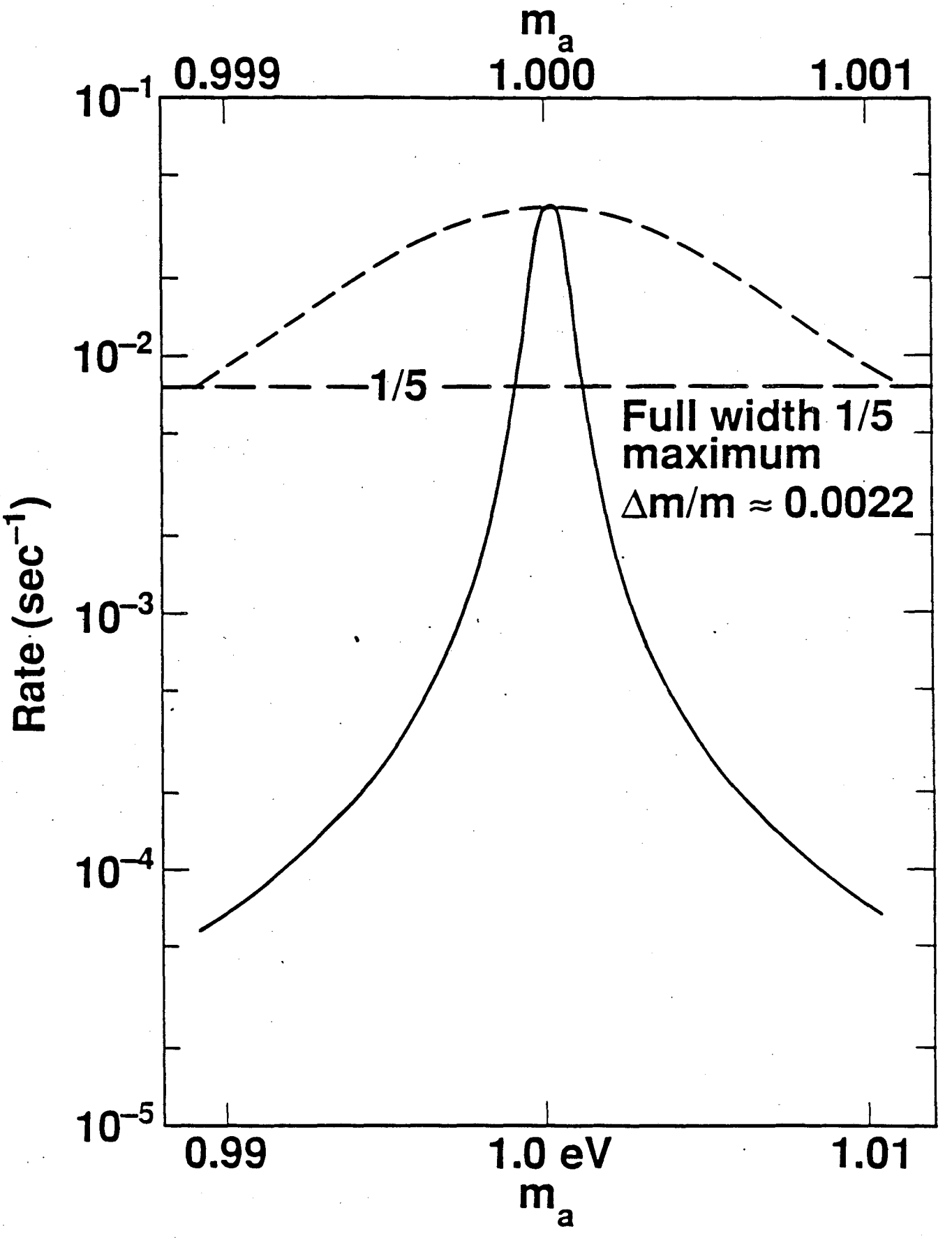
m_a
0.999
1.000
1.001
10^-1
10^-2
10^-3
10^-4
10^-5
1/5
Full width 1/5 maximum
Δm/m ≈ 0.0022
Rate (sec^-1)
0.99
1.0 eV
1.01
m_a

Figure 5

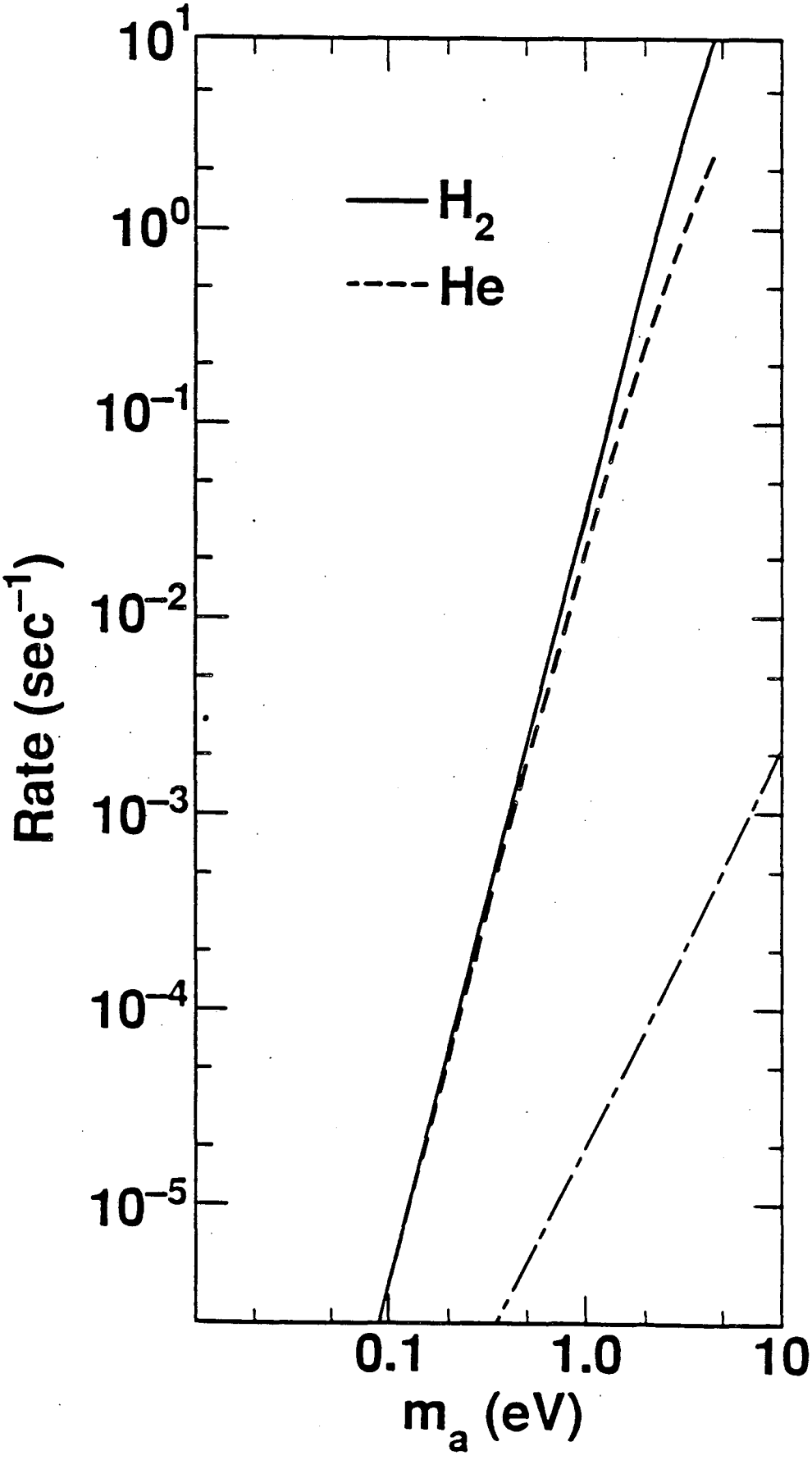

Figure 6

AM-136-U-5465-9

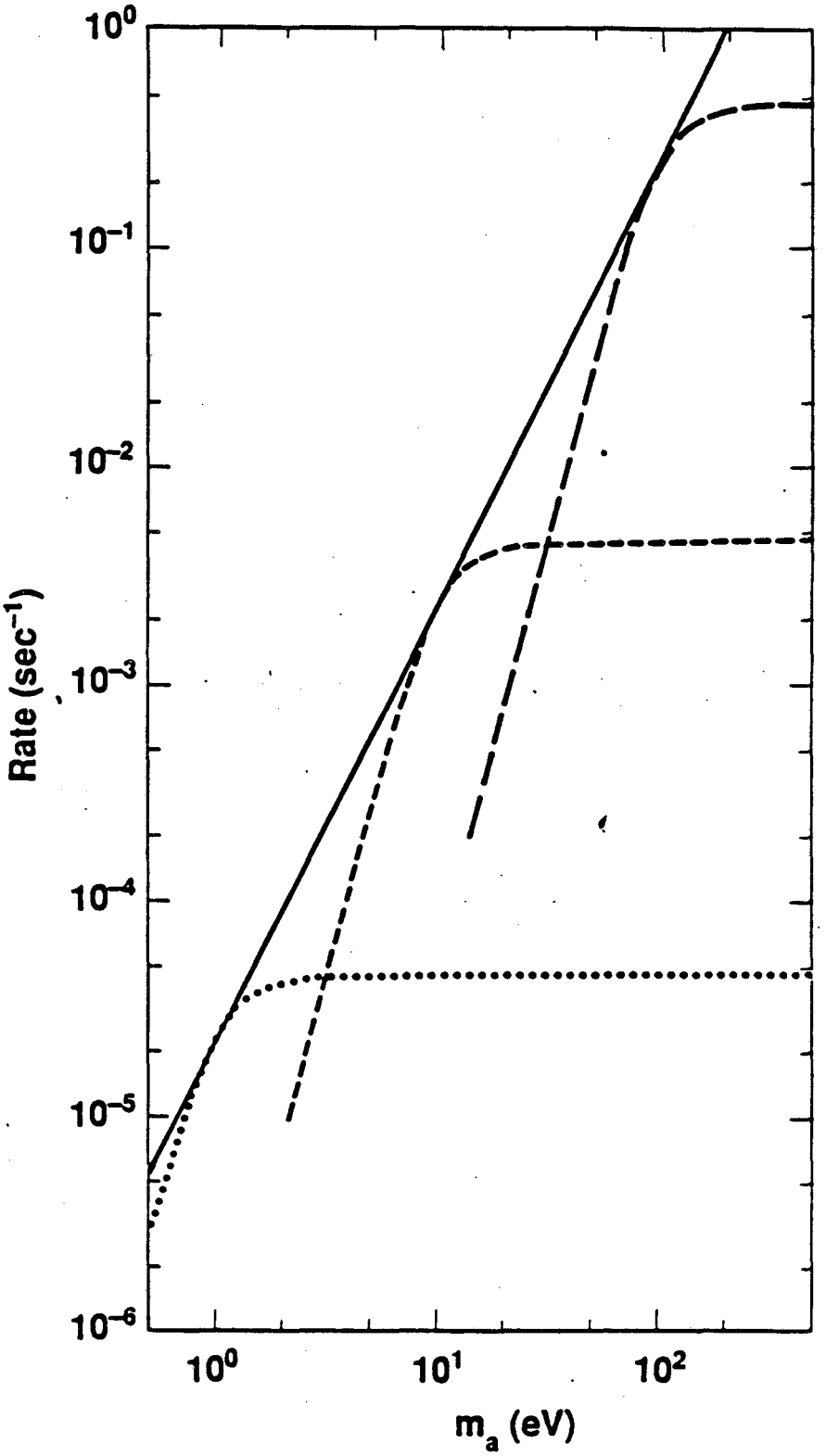

Figure 7

LAWRENCE BERKELEY LABORATORY
TECHNICAL INFORMATION DEPARTMENT
UNIVERSITY OF CALIFORNIA
BERKELEY, CALIFORNIA 94720